Synthesis, biophysical characterization and anti-HIV activity of d(TG₃AG) Quadruplexes bearing hydrophobic tails at the 5′-end

CrossMark

Valeria Romanucci [a], Danilo Milardi [b], Tiziana Campagna [b], Maria Gaglione [c], Anna Messere [c], Alessandro D'Urso [d], Emanuela Crisafi [d], Carmelo La Rosa [d], Armando Zarrelli [a], Jan Balzarini [e], Giovanni Di Fabio [a,*]

[a] Department of Chemical Sciences, University of Napoli 'Federico II', Via Cintia 4, I-80126 Napoli, Italy
[b] Istituto di Biostrutture e Bioimmagini—Catania, Consiglio Nazionale delle Ricerche, Viale Andrea Doria 6, 95125 Catania, Italy
[c] Dipartimento di Scienze e Tecnologie Ambientali, Biologiche e Farmaceutiche, Seconda Università di Napoli, Via Vivaldi 43, 81100 Caserta, Italy
[d] Dipartimento di Scienze Chimiche, Università degli Studi di Catania, Viale Andrea Doria 6, 95125 Catania, Italy
[e] Rega Institute for Medical Research, KU Leuven, Minderbroedersstraat 10, B-3000 Leuven, Belgium

ARTICLE INFO

ABSTRACT

Novel conjugated G-quadruplex-forming d(TG₃AG) oligonucleotides, linked to hydrophobic groups through phosphodiester bonds at 5′-end, have been synthesized as potential anti-HIV aptamers, via a fully automated, online phosphoramidite-based solid-phase strategy. Conjugated quadruplexes showed pronounced anti-HIV activity with some preference for HIV-1, with inhibitory activity invariably in the low micromolar range. The CD and DSC monitored thermal denaturation studies on the resulting quadruplexes, indicated the insertion of lipophilic residue at the 5′-end, conferring always improved stability to the quadruplex complex $(20 < \Delta Tm < 40\ °C)$. The data suggest no direct functional relationship between the thermal stability and anti-HIV activity of the folded conjugated G-quartets. It would appear that the nature of the residue at 5′ end of the d(TG₃AG) quadruplexes plays an important role in the thermodynamic stabilization but a minor influence on the anti-HIV activity. Moreover, a detailed CD and DSC analyses indicate a monophasic behaviour for sequences **I** and **V**, while for ODNs (**II–IV**) clearly show that these quadruplex structures deviate from simple two-state melting, supporting the hypothesis that intermediate states along the dissociation pathway may exist.

© 2014 Elsevier Ltd. All rights reserved.

1. Introduction

The chemical nature of nucleic acids provides a variety of specific and biologically relevant interactions with different classes of biomolecules.[1–4] Aptamers are DNA sequences that can bind selectively and specifically to target molecules. Their small size, straightforward synthesis, and flexibility make aptamers advantageous over other molecules, such as antibodies. The structure and conformation of aptamers can be rationally designed and tailor-made for various types of targets.

Recently, the use of synthetic nucleic acids to modulate the activities of proteins for therapeutic purposes has received major attention. In this field, G-rich oligonucleotides (GROs), which are able to form G-quadruplexes, have attracted considerable interest.[5–8] GROs are among the most studied DNA structures because they are thought to be involved in important biological processes such as the modulation of gene expression resulting by protein recognition of G-quadruplex structures. They also show promising

biological properties ranging from anticancer to antiviral activities. In all cases, G-quadruplex formation is a crucial prerequisite for these biological effects.[9,10]

Many G-quadruplex forming oligonucleotides have been found to be potent antiviral agents, and a number of these agents has been modified and selected as promising drug candidates against HIV (human immunodeficiency virus).[11–15] Two mechanisms have been proposed to explain the antiviral activity of G-rich oligomers: the inhibition of viral entry into the cell via interaction with the positively charged V3 loop of the gp120 envelope protein (primary target), and/or the inhibition of the HIV-1-encoded integrase (secondary target). The first G-quadruplex forming oligonucleotide to exhibit potent anti-HIV activity was the 8-mer d(T₂G₄T₂), which was shown to bind to the V3 loop of the envelope protein gp120 and inhibit virus adsorption and cell fusion.[16] Recently, several short G-quadruplexes have been evaluated as potential anti-HIV drug candidates, due to their binding with proteins related for the HIV-1 infection. The intramolecular or intermolecular quadruplex structural motifs were thought to be essential to anti-HIV activity.[12,13,17–25]

* Corresponding author. Tel.: +39 081 674001; fax: +39 081 674393.
E-mail address: difabio@unina.it (G. Di Fabio).

The sequence d(TG₃AG), also known as Hotoda's sequence, was conjugated to a variety of aromatic groups at the 5′-end and tested for activity against HIV-1.[26–28] While the unmodified quadruplex d(TG₃AG) had no anti-HIV-1 activity, quadruplexes carrying aromatic groups at the 5′-end inhibited HIV-1 with low cytotoxicity. In particular, the d(TG₃AG) quadruplex forming ODNs bearing a 3,4-dibenzyloxybenzyl group at the 5′-ends and 2-hydroxyethyl-phosphate at the 3′-ends (R-95288) showed the highest anti-HIV activity. Spectroscopic studies suggested that 5′-conjugated d(TG₃AG) formed parallel tetramolecular quadruplex structures. The synthesis and the structure–activity relationship of novel modified

Hotoda's sequences[29–32] have become the focus of many studies because of their pharmaceutical potential.

To explore the relationship between the structure of these G-rich ODNs and their activity, we analysed some representative anti-HIV Hotoda's 6-mers and compared them with unmodified d(TG₃AG).[33,34] Based on previous studies, we hypothesised that the aromatic groups at the 5′-end are crucial for the stability of the G-quadruplex, dramatically enhancing both the rate of formation and the thermodynamic stability of the quadruplex complexes and therefore their anti-HIV activity. Recently, we described a general approach to generating a mini library of new d(TG₃AG) ODNs,
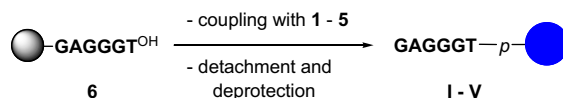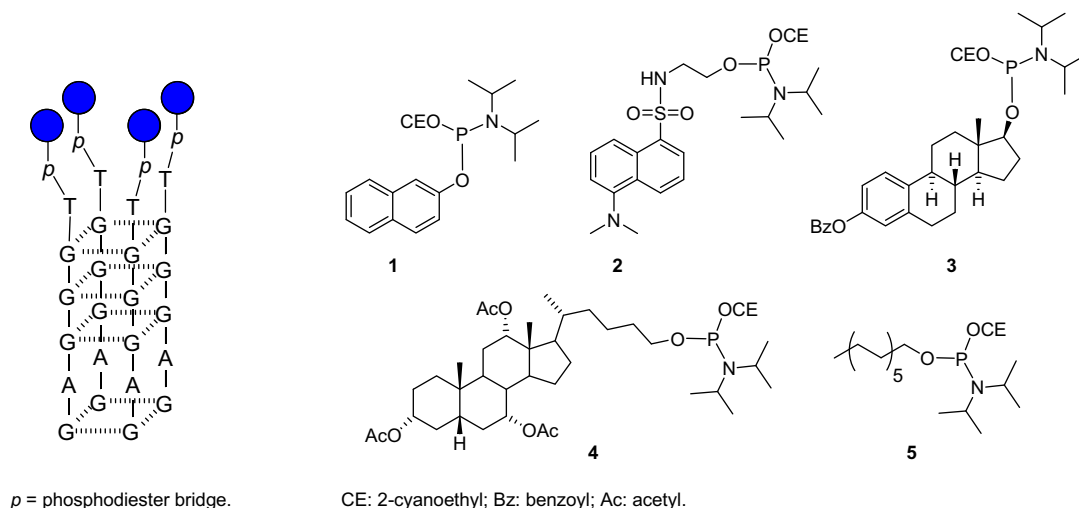

p = phosphodiester bridge.

CE: 2-cyanoethyl; Bz: benzoyl; Ac: acetyl.

Figure 1. Phosphoramidite building blocks **1**–**5** and synthetic scheme for the preparation of conjugated oligonucleotides **I**–**V**.

Table 1
Oligonucleotide Characterization

Sequence (5′–3′)	MS calcd for [M] data (found)
I	2077.37 2078.64 [MH]⁺ 2101.23 [MNa]⁺
II	2227.42 2228.25 [MH]⁺ 2250.84 [MNa]⁺
III	2205.49 2206.54 [MH]⁺ 2228.28 [MNa]⁺
IV	2341.64 2342.59 [MH]⁺ 2365.87 [MNa]⁺ 2380.46 [MK]⁺
V	2119.51 2120.46 [MH]⁺ 2145.21 [MNa]⁺

ᵃFor HPLC conditions see paragraph 4.3.

conjugated to different aromatic groups at the 5′-end through a phosphodiester bond.[35] Several modified sequences showed significant anti-HIV-1 activity and high binding affinity for the HIV-1 envelope proteins gp120 and gp41. CD analyses showed that the residues at the 5′-end in these structures played a principal role on the G-quadruplex stability by enhancing thermodynamic stability (ΔTm >20 °C).

Given the importance of G-tetraplex forming ODNs as potent anti-HIV inhibitors, we aimed to conjugate suitable molecules able to stabilise quadruplexes through aromatic and non-aromatic interactions. To extend the number of modified G-rich ODNs and to perform a detailed study of the structure–activity relationship, we synthesised and biophysically and biologically characterised a mini-library of new d(TG₃AG) oligomers **I–V** carrying hydrophobic and groups at the 5′-end by a phosphodiester bond. Some of the groups are known for their ability to improve cellular uptake, extend the half-life of these molecules in plasma, or stabilise DNA structures through hydrophobic interactions.[36–39]

Detailed CD analysis and thermal denaturation DSC/CD studies for the 5′-conjugated d(TG₃AG) **I–V** were carried out and discussed. To examine the structure–activity relationship, ODNs **I–V** were evaluated for their anti-HIV activity and their affinity for HIV envelope proteins gp120, gp41 and human serum albumin (HSA).

2. Results and discussion

Based on Hotoda's sequence, d(TG₃AG), a small library of 5′-conjugates carrying aromatic, hydrophobic, amphiphilic, fluorescent groups was synthesised and purified. Initially, the scaffold **6** (Fig. 1) was synthesised using standard solid phase β-cyanoethyl phosphoramidite chemistry protocols starting from a commercially available DMT-protected guanosine functionalised CPG support.[40] Phosphoramidite derivatives **1–5** (Fig. 1) were exploited in the last coupling step to synthesise the 5′-conjugated oligomers **I–V** (Fig. 1 and Table 1).

CD spectroscopy can be used to obtain details about the quadruplex structures by comparing their spectra with those of quadruplex DNAs with known conformations.[41] Figure 2 shows the CD spectra of the five oligonucleotides at temperatures ranging from 15 to 90 °C in the same buffer conditions.

The CD spectra of all five sequences recorded at 15 °C show a positive peak at 260 nm and a small negative band around 240 nm.

These spectral shapes are consistent with the reported spectra of other TG₃AG sequences[33] and clearly indicate that all of the strands fold into an all-parallel-stranded structure. The melting temperature values (Table 2) were determined from the CD melting profiles for conjugates **I–V** monitored at 263 nm with an heating rate of 1 °C/min, (Fig. 3, bottom). In Figure 3 (top), the DSC results from the same samples used in the CD melting experiments are presented.

A direct comparison of the CD and DSC data obtained for identical samples can be used to rule out the possibility of incompletely formed quadruplexes before heating and provide a more detailed description of the thermal transitions. All heating runs were fully irreversible. Therefore, neither an extrapolation of the thermodynamic parameters ΔG and ΔS from the melting curves nor a deconvolution of the Cp curves by statistical mechanic methods were possible.[38] For compound **I**, DSC runs exhibited a broad monophasic peak centred at $T_m = 60$ °C and $\Delta H_{cal} = 314$ kJ mol⁻¹, which indicates the formation of four G-tetrads, as reported elsewhere.[30] The melting temperature of compound **I** derived from the DSC curves was 4 °C higher than that obtained from the CD results. This difference in the melting temperatures may be ascribed to the asymmetry of the calorimetric trace. The CD melting curve of compound **II** shows biphasic behaviour with a first melting point centred at 46 °C and a second one observed at 71 °C. The corresponding DSC

curve shows a large asymmetric peak with a maximum at 73 °C and a small shoulder at 46 °C. The overall calorimetric enthalpy of this peak is 305 kJ mol⁻¹. Biphasic behaviour is observed in the CD melting curve of compound **III**; the first transition is observed at 33 °C, and the second transition is observed at 79 °C. The DSC curve of compound **III** shows an endothermic peak at 33 °C corresponding to the CD transition and a second, distinct peak at 89 °C. The calorimetric enthalpies for these two transitions are 15 and 124 kJ mol⁻¹, respectively. The CD melting profile of compound **IV** exhibits biphasic behaviour, with the first transition at 45 °C and a second transition at 79 °C.
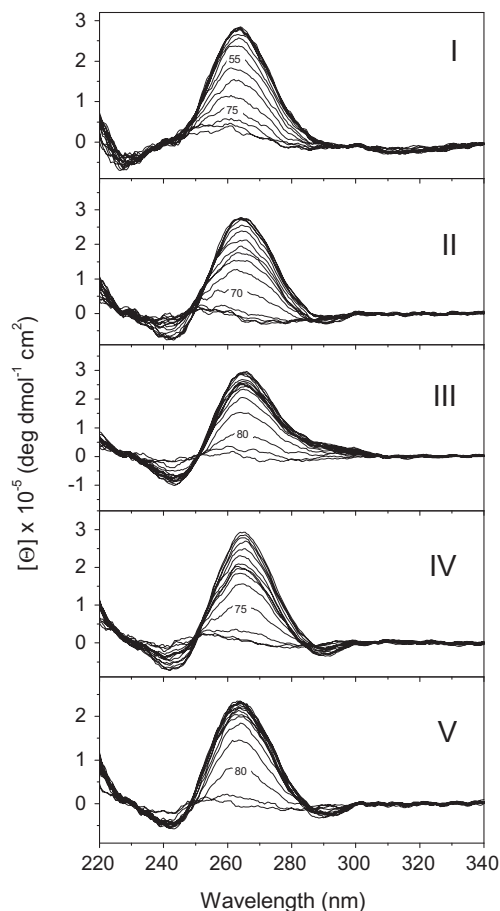

Figure 2. CD spectra of **I–V**. The spectra were collected at 15 °C and at steps of 5 °C up to 90 °C in a 10 mM potassium phosphate buffer (pH 7.0), supplemented with 200 mM KCl, at 10 μM of single strand. To guide the eye throughout the figures, some representative curves are marked with the temperature at which the CD signal was recorded.

Table 2
Thermodynamic parameters for the thermally-induced Quadruplex dissociation[a]

	CD		DSC			
	T_m (°C) ± 1		T_m (°C) ± 1		$\Delta H°_{cal}$ (KJmol⁻¹)	
	1st	2nd	1st	2nd	1st	2nd
I	nd	56	nd	61	nd	314 ± 15
II	46	71	46	74	nd	305 ± 10
III	33	79	33	90	15 ± 5	124 ± 11
IV	45	79	45	81	24 ± 15	252 ± 15
V	nd	76	nd	84	nd	182 ± 10

[a] The same sample was splitted in two parts used in parallel for CD and DSC analysis.
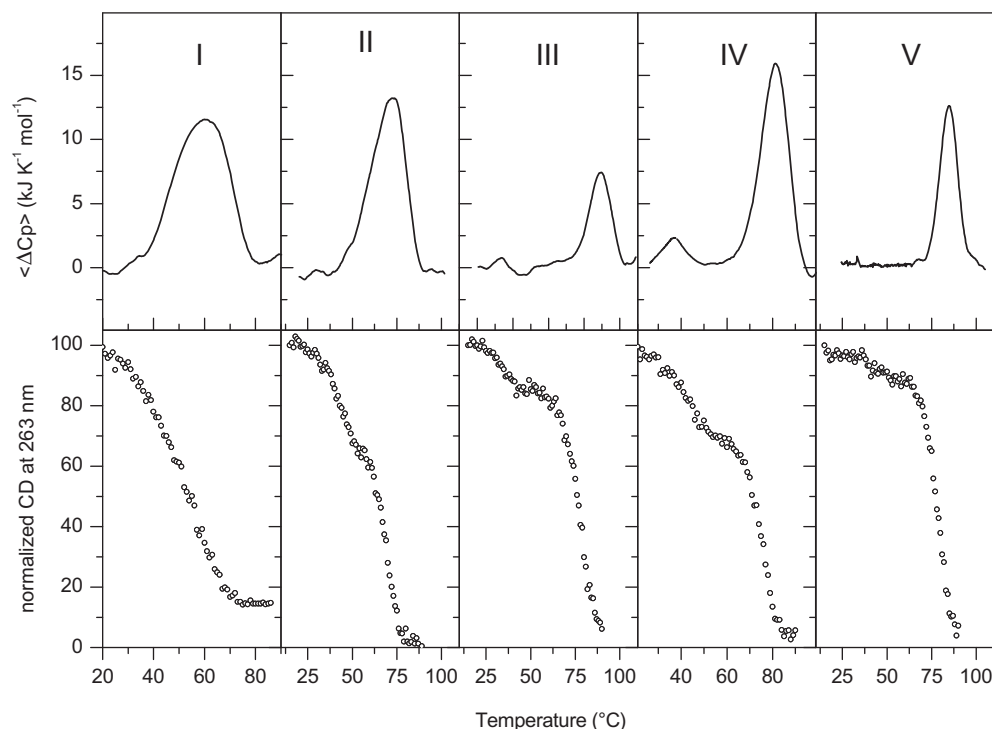
Figure 3. DSC (top) and CD (bottom) melting profiles of **I–V**.

Table 3
Antiviral (HIV) and RT activities of test compounds in CEM cell cultures

Sequences	EC$_{50}$[a] (μM)		IC$_{50}$[b] (μM)
	HIV-1(III$_B$)	HIV-2(ROD)	RT (Pol.rC.dG)
I	>8	68 ± 18	n.d.
II	9.9 ± 4.4	31 ± 0.0	>30
III	4.8 ± 0.3	6.6 ± 1.9	2.5 ± 0.63
IV	6.8 ± 1.8	12 ± 9.7	>30
V	5.3 ± 0.2	⩾8	6.72 ± 0.48

[a] 50% Effective concentration or compound concentration required to inhibit HIV-induced cytopathicity by 50% in CEM cell cultures.
[b] 50% inhibitory concentration required to inhibit the RT reaction by 50%.

Table 4
Interaction of the quadruplex derivatives with viral and human (glyco)proteins

Sequences	Amplitude of the SPR signal[a] (RU)		
	HIV-1 gp120	HIV-1 gp41	HSA[b]
II	0.4	4.0	13
III	8.7	28	45
IV	4.7	35	6.0
V	0.1	21	21

[a] Amplitude of the SPR signal was measured after 120 s exposure of the compounds to the (glyco)proteins.
[b] Human Serum Albumin.

The corresponding DSC curve shows an initial, smaller peak at 45 °C and a second peak at 81 °C. The calorimetric enthalpies for the two transitions are 24 and 252 kJ mol^{-1}, respectively. Finally, the CD melting profile of compound **V** shows a single transition at 76 °C. The DSC curve of compound **V** shows monophasic behaviour, with an endothermic peak centred at 84 °C with a calorimetric enthalpy of 188 kJ mol^{-1}. Several research groups have reported that modified G-quadruplex d(TG$_3$AG) sequences are stabilised at increasing melting temperatures relative to the parent unmodified

sequence. Our results (Table 2) are consistent with these reports; however, we found that the melting of many of these structures is not a simple two-state process, as assumed in previous studies. Although the irreversible nature of the melting processes of the studied assemblies made a thorough analysis of the <ΔCp> curves in thermodynamic terms difficult, our integrated CD and DSC dissociation studies provide a better understanding of the complexities in the melting mechanism. The CD melting data for compounds **II**, **III** and **IV** clearly show that these quadruplex structures deviate from a simple two-state melting and support the hypothesis that intermediate states along the dissociation pathway may exist. Such complex behaviour is consistent with the analysis of the DSC thermograms. However, the existence of intermediates along the broad melting curve of compound **I** cannot be excluded. It should be noted that the folding/unfolding reactions of G-Quadruplexes are almost always assumed for convenience to be two-state processes, with negligible concentrations of any intermediate species along the melting pathway. However, a number of studies have revealed that in both Na$^+$ and K$^+$ solutions, multiple conformations may coexist.[42–45] A thermally dependent equilibrium between two G-quadruplex isoforms with different stabilities would explain the biphasic melting curves observed. Lower thermal stability is generally attributed to flanking interstrand contacts at the edges of the G-Quadruplex structures.

Compounds **I–V** were evaluated for their anti-HIV-1 and -HIV-2 activities in CEM cell cultures (Table 3). All compounds showed pronounced anti-HIV activities, with some preference for HIV-1. This inhibitory activity (except compound **I**) was invariably in the low micromolar range (50% effective concentration (EC$_{50}$: 4.9–10 μM for HIV-1 and 6.7–32 μM for HIV-2). Compound **I** was clearly less inhibitory (EC$_{50}$ >8 μM for HIV-1 and 69 μM for HIV-2). A concentration higher than 8 μM could not be microscopically scored due to unexplained toxicity in the HIV-1-infected (but not HIV-2-infected) CEM cell cultures. In light of the thermodynamic data and biological activity, it is reasonable to conclude that the nature of the 5′-end modification on the d(TG$_3$AG) quadruplexes

played only a minor role in the anti-HIV activity. Because the conjugated quadruplexes may inhibit HIV entry into its target cells due to their negative charge, conjugates **II**–**V** were also evaluated for their affinity to HIV envelope gp120 and gp41, as well as HSA as a control, by surface plasmon resonance (SPR) technology (Table 4) and for their inhibitory effect against HIV-1 reverse transcriptase (RT). The biosensor chips for the SPR analyses were loaded with 3531 RU gp120, 3091 RU gp41, or 3333 RU HSA and exposed to 1 OD/ml of the compounds. A binding signal was recorded for each of the compounds against the three proteins.

However, the binding amplitudes measured after compound exposure to the protein for 120 s differed significantly depending on the nature of the compound and the glycoprotein evaluated. The compounds **III** and **IV** showed a clear binding capacity (amplitude range: 4.7–8.7 RU) to gp120 whereas **II** and **V** showed poor, if any binding. Compounds **III**, **IV** and **V** were by far superior for binding to gp41, and compound **III** showed the strongest binding to HSA (Table 4 and Supporting Informations).

Compounds **III** and **V** bound to HSA better than to gp41. In the HIV-1 RT experiments, **II**, **III**, **IV** and **V** showed varying inhibitory activities (**I** was not evaluated). Their IC_{50} values were in the range 2.5–69 μM, respectively, when using poly rC.dG as the template/primer and radiolabeled [³H]dGTP as the substrate (Table 3).

Considering all of the SPR data, there does not appear to be any selectivity for gp120 or gp 41 binding compared with HSA binding. Also, no correlation between anti-HIV-1 and anti-RT activity was found. Therefore, it remains unclear whether selective binding to the HIV envelope or RT inhibition represents a mechanism for the selective antiviral action of these conjugates.

The affinity of the synthetic oligonucleotides (**II**–**V**) for HSA is an interesting finding because the use of albumin as a versatile drug carrier in anti-HIV strategy is increasing. In fact, many albumin-based formulations have received market approval or are being evaluated in clinical trials.[46,47] In light of these results, it would be interesting to investigate the ability of all active 5′-end conjugated d(TG₃AG) to bind HSA.

3. Conclusions

In conclusion, new d(TG₃AG) ODNs carrying aromatic, hydrophobic, amphiphilic and fluorescent tails at the 5′-end via a phosphodiester bond were synthesized as potential anti-HIV agents via a fully automated, on-line phosphoramidite-based solid-phase method. The compounds **I**–**V** showed enhanced anti-HIV activity with some selectivity for HIV-1. The new compounds have also been evaluated for their affinity to the HIV envelope glycoproteins gp120 and gp41 and human serum albumin by SPR and for their inhibition of HIV-1-encoded reverse transcriptase. The compounds **III** and **V** showed almost equal binding capacity to gp120 whereas compounds **III**, **IV** and **V** were superior to **II** for binding to gp41, and compound **III** showed strongest binding to HSA. Moreover, compound **III** bound to HSA better than to gp41. DSC and CD analyses were carried out for the conjugates **I**–**V** and revealed diagnostic profiles of parallel-stranded quadruplex structures for all of the sequences studied. While the CD and DSC analyses for sequences **I** and **V** indicated monophasic behavior with an endothermic peak, the results for compounds **II**–**IV** clearly showed that these quadruplex structures deviate from a simple two-state melting and support the hypothesis that intermediate states along the dissociation pathway may exist. As already reported, we can conclude that the formation of quadruplex structures for modified G-rich oligonucleotides appears to be necessary for their antiviral activity. An in-depth analysis is required to understand the role of conjugating molecules. Structural characterization studies combining kinetic analysis with molecular modeling of the ODNs presented here and in previous work[35] are currently underway in our

laboratories to obtain a more complete picture of their structure–activity relationships, which will be useful for the design of new conjugated G-quadruplexes as aptamers.

4. Exprimental procedures[†]

4.1. General procedures

Starting compounds for the synthesis of phosphoramidites **1**–**5** were all purchased from Sigma–Aldrich. TLC analyses were carried out on silica gel plates from Merck (Kieselgel 60, *F254*). Reaction products were visualized on TLC plates by UV light and then by treatment with a H_2SO_4/AcOH aqueous solution. For column chromatography, silica gel from Merck (Kieselgel 40, 0.063–0.200 mm) was used. NMR spectra were recorded in $CDCl_3$ with a Bruker WM 400 spectrometer. The chemical shifts (δ) are given in ppm with respect to the residual solvent signal (7.26 ppm), and the coupling constants (J) are in Hz. ³¹P NMR spectra were recorded at 161.98 MHz on a Bruker WM-400 spectrometer using 85% H_3PO_4 as an external standard. MALDI TOF mass spectrometric analyses were performed on a PerSeptive Biosystems Voyager—De Pro MALDI mass spectrometer in the linear mode using a picolinic/3–hydroxypicolinic/sinapinic acid mixture as the matrix. For the ESI MS analyses, a Waters Micromass ZQ instrument equipped with an Electrospray source was used in the positive mode. HPLC analyses were performed on an Agilent Technologies 1200 series instrument equipped with a UV detector. The crude material was analysed and purified by HPLC on a Nucleogel SAX column (Macherey–Nagel, 1000–8/46) or Phenomenex RP18 column [LUNA, 5 μm C18(2), 10.0 × 250 mm]. Desalting was carried out by gel filtration chromatography on a Sephadex G25 column eluted with H_2O/EtOH 4:1 (v/v).

4.2. General procedure for the Preparation of Phosphoramidite 1–5

1.26 mmol of alcohol was dissolved in 10 mL of anhydrous dichloromethane, and 880 μL DIPEA (5.05 mmol) and 565 μL 2-cyanoethyl-*N*,*N*-diisopropylamino-chlorophosphoramidite (2.52 mmol) were added under argon. After 30 min, the solution was diluted with ethyl acetate, and the organic phase was washed twice with brine and then concentrated. Silica gel chromatography of the residue (eluent hexane/ethyl acetate) afforded the desired compounds (**1**–**5**).

1 ¹H NMR ($CDCl_3$, 400 MHz, 20 °C, mixture of enantiomers): δ 7.58 (3H, overlapped signals, H-4, H-8 and H-5), 7.15 (2H, overlapped signals, H-7 and H-9), 7.17 (1H, m, H-1), 7.04 (1H, d, J = 8.5 Hz, H-3), 3.73 (2H, m, OCH_2CH₂CN), 3.56 (2H, m, N[CH(CH₃)₂]₂), 2.46 (2H, t, J = 8.0 Hz, OCH₂CH_2CN), 1.04 (6H, d, J = 8.0 Hz, N[CH(CH_3)₂]₂), 0.98 (6H, d, J = 8.0 Hz, N[CH(CH_3)₂]₂); ¹³C NMR ($CDCl_3$, 75 MHz): δ. 151.8, 134.0, 129.5, 129.1, 127.4, 126.8, 126.0, 124.0, 121.1, 117.4, 114.7, 58.7, 43.4, 24.2, 24.0, 20.3, 19.9. ³¹P NMR ($CDCl_3$, 161.98 MHz): δ 149.2. ESI–MS: calculated for $C_{20}H_{26}NO_2P$ 343.17. Found (positive ions): 344.26 (M−H)⁺.

2 ¹H NMR ($CDCl_3$, 400 MHz, 20 °C, mixture of enantiomers): δ 8.53 (1H, d, J = 8.4 Hz), 8.30 (1H, d, J = 8.4 Hz), 8.24 (1H, d, J = 7.2 Hz), 7.53 (2H, m), 7.18 (1H, d, J = 7.6 Hz), 3.75–3.44 (6H, overlapped signals, OCH_2CH₂CN, NHCH₂CH_2O and N[CH(CH₃)₂]₂), 3.08 (2H, m, NHCH_2CH₂O), 2.86 (6H, s, NCH_3), 2.55 (2H, m, OCH₂-CH_2CN), 1.25 (6H, d, J = 6.6 Hz, N[CH(CH_3)₂]₂), 1.04 (6H, d, J = 6.7 Hz, N[CH(CH_3)₂]₂). ¹³C NMR ($CDCl_3$, 75 MHz): δ 151.9, 130.3, 129.7, 129.4, 128.3, 123.1, 119.6, 118.6, 117.6, 115.1, 62.2,

---

58.3, 45.3, 44.1, 42.9, 24.4, 20.1. ^{31}P NMR (CDCl$_3$, 161.98 MHz): δ 151.7. ESI–MS: calculated for C$_{34}$H$_{61}$N$_2$O$_5$P 608.43. Found (positive ions): 609.51 (M−H)$^+$.

3 ^{1}H NMR (CDCl$_3$, 400 MHz, 20 °C, mixture of diastereoisomers): δ 8.23 (2H, d, J = 7.6 Hz), 7.63 (1H, t, J = 7.6 Hz), 7.51 (2H, t, J = 7.6 Hz), 7.33 (1H, dd, J = 8.4, 3.2 Hz), 6.97 (1H, d, J = 8.4 Hz), 6.93 (1H, s), 3.80–3.76 (3H, complex signal, OCH_2CH$_2$CN, H-17 of β–estradiol residue), 3.64–3.58 (2H, complex signal, N[CH(CH$_3$)$_2$]$_2$). ^{13}C NMR (75 MHz, CDCl$_3$): δ 165.4, 148.6, 138.3, 138.1, 133.4, 130.1, 129.6, 128.5, 126.4, 121.6, 118.6, 117.8, 83.7, 82.5, 58.4, 57.8, 49.7, 44.1, 43.5, 42.9, 38.4, 37.2, 36.9, 29.6, 26.9, 26.1, 24.6, 23.2, 20.4, 11.9, 11.7. ^{31}P NMR (161.98 MHz, CDCl$_3$): δ 150.5, 149.5. ^{31}P NMR (CDCl$_3$, 161.98 MHz): δ 150.5, 149.5. ESI–MS: calculated for C$_{27}$H$_{41}$N$_2$O$_3$P 473.29. Found (positive ions): 474.69 (M−H)$^+$.

4 ^{1}H NMR (CDCl$_3$, 400 MHz, 20 °C, mixture of diastereoisomers): δ 5.02 (1H, br s), 4.90 (1H, br s), 4.58 (1H, m), 4.09 (2H, t, J = 5.0 Hz), 3.80 (2H, complex signals), 3.58 (4H, complex signals), 2.63 (2H, t, J = 6.3 Hz), 2.13 (3H, s), 2.08 (3H, s), 2.05 (3H, s), 1.95–0.65 (45H, complex signals). ^{13}C NMR (CDCl$_3$, 75 MHz): δ 169.0, 169.1, 168.7, 74.2, 73.0, 69.2, 63.8, 60.2, 48.5, 47.6, 43.3, 43.1, 42.3, 41.2, 40.6, 37.2, 36.6, 36.0, 33.4, 31.3, 30.8, 30.5, 29.7, 28.9, 28.0, 25.4, 24.4, 23.3, 23.0, 20.02, 18.2, 13.1. ^{31}P NMR (CDCl$_3$, 161.98 MHz): δ 151.7, 150.7. ESI–MS: calculated for C$_{33}$H$_{59}$N$_2$O$_5$P 594.42 Found (positive ions): 595.32 (M−H)$^+$.

5 ^{1}H NMR (CDCl$_3$, 400 MHz, 20 °C, mixture of enantiomers): δ 3.80 (2H, m, OCH_2CH$_2$CN,), 3.58 (4H, complex signals, N[CH(CH$_3$)$_2$]$_2$, OCH$_2$CH$_2$(CH_2)$_9$CH$_3$), 2.63 (2H, t, J = 6.3 Hz, OCH$_2$-CH_2CN), 1.56 (2H, m, OCH$_2$CH$_2$(CH_2)$_9$CH$_3$), 1.34–1.12 (30H, m, N[CH(CH_3)$_2$]$_2$, OCH$_2$CH$_2$(CH_2)$_9$CH$_3$), 0.87 (3H, t, J = 6.0 Hz). ^{13}C NMR (CDCl$_3$, 75 MHz): δ 119.4, 63.7, 58.3, 42.9, 31.9, 31.2, 29.8, 29.6, 29.5, 26.1, 24.5, 22.6, 20.3, 14.0. ^{31}P NMR (CDCl$_3$, 161.98 MHz): δ 152.9. ESI–MS: calculated for C$_{21}$H$_{43}$N$_2$O$_2$P 386.31. Found (positive ions): 387.55 (M−H)$^+$.

4.3. Synthesis and Characterisation of ODNs (I–V)

As depicted in Figure 1, oligomers **I–V** were synthesised, starting from functionalised CPG support **6** with 0.07–0.08 meq/g initial loading, on which the sequence d(TG$_3$GAG) was assembled in a standard manner. Starting with 100 mg of commercially available CPG-dG support with 0.10 meq/g initial loading, and after the assembly of the sequence d(TGGGA), an additional coupling with phosphoramidite building blocks **1–5** was then performed. Target oligomers **I–V** were detached from the solid support and deprotected by treatment with Et$_3$N/pyridine (1:1, v/v) at 50 °C for 1 h, followed by treatment with conc. aq. ammonia at 50 °C for 5 h. The combined filtrates and washings were concentrated under reduced pressure, re-dissolved in H$_2$O, and analysed and purified by HPLC. Purification of the crude conjugated oligonucleotides **I–V** was carried out on Phenomenex RP18 column or RP18 column (LUNA, 5 μm C18(2), 10.0 × 250 mm) using a linear gradient of CH$_3$CN in 0.1 M AcNH$_4$ in H$_2$O, pH 7.0 from 5% to 100% over 30 min at a flow rate of 1.5 mL/min with detection at 260 nm. In all cases 50–80 OD units of pure **I–V** could be on average recovered starting from 100 mg of functionalized solid support (average yields 16–25%).

4.4. Quadruplexes preparation

The quadruplex complexes were obtained by dissolving the lyophilized oligonucleotide at a single strand concentration of 1×10^{-4} M in the appropriate buffer. The solution was then annealed by heating at 90 °C for 5 min and slow cooling to room temperature. The buffer used was 10 mM potassium phosphate, 200 mM KCl, 0.1 mM EDTA at pH 7.0. The concentration of the dissolved oligonucleotides **I–V** was determined by UV measurements at 260 nm and at 95 °C, using, as the molar extinction coefficients, the values calculated by the nearest neighbor model for the sequence d(TG$_3$AG), and the values experimentally calculated for labels **1–3** (808, 1083, and 703 cm^{-1} M^{-1}, respectively).

4.5. CD experiments

CD spectra were recorded by a JASCO J-810 spectropolarimeter equipped with a thermostatically controlled accessory (JASCO PTC-348), using a quartz cuvette with a 0.5 cm optical path. CD spectra were collected from 220 to 340 nm, at 20 nm/min, with a response time of 4 s and at 1 nm bandwidth. The CD signal of the buffer was subtracted from all CD spectra, corresponding to an average of 5 scans. The molar ellipticity was calculated by the equation $[\theta] = 100 \times \theta/cl$ where θ is the ellipticity value, c is the concentration of the single strand (1.0×10^{-5} M), and l is the path length of the cell in cm. The thermally-induced dissociation of the quadruplexes was studied by monitoring the CD signal at 263 nm upon increasing the temperature from 15 to 90 °C (heating rate = 1 °C/min). The melting temperatures were calculated from the peaks of the first derivative of the CD signal vs T.

4.6. DSC experiments

DSC runs were all performed by a VP-DSC calorimeter (MicroCal). All samples, after a degassing process, were scanned at a heating rate of 1 °C min^{-1} in the temperature range 20–120 °C in the same experimental conditions adopted for the CD experiments. An extra external pressure of about 29 psi was applied to the solution to prevent the formation of air bubbles during heating. To ensure a complete equilibration of the calorimeter, several buffer–buffer heating scans were routinely performed prior to the measurement. Only after obtaining invariant buffer–buffer baselines samples were scanned. Additional buffer–buffer baselines were obtained immediately after the protein scans to double-check for uncontrolled drifts in instrumental baseline. For each sample, three independent DSC experiments were carried out under the same buffer conditions. To obtain the heat capacity Cp curves, buffer–buffer base lines were recorded at the same scanning rate and then subtracted from sample curves, as previously described.[48] In all experiments, one or several heating–cooling cycles were carried out to determine the reversibility of the denaturation process. To obtain the excess heat capacity profiles <ΔCp>, the DSC curves, after instrumental baseline correction, were subtracted from a baseline obtained by a third-order polynomial fit of the pre- and post-transition Cp trends as reported elsewhere.[49–51] Melting temperatures were calculated from the maximum Cp value of the DSC curve.

4.7. Anti-HIV experiments

Inhibition of HIV-1(III$_B$)- and HIV-2(ROD)-induced cytopathicity in CEM cell cultures was measured in microliter 96-well plates containing ~3×10^5 CEM cells/mL infected with 100 CCID50 of HIV per milliliter and containing appropriate dilutions of the test compounds. After 4–5 days of incubation at 37 °C in a CO$_2$-controlled humidified atmosphere, CEM giant (syncytium) cell formation was examined microscopically. The EC$_{50}$ (50% effective concentration) was defined as the compound concentration required to inhibit HIV-induced giant cell formation by 50%.

4.8. Surface plasmon resonance (SPR) analysis

Interaction studies were performed on a Biacore T200 instrument (GE Healthcare, Uppsala, Sweden) at 25 °C in HBS-P (10 mM HEPES, 150 mM NaCl and 0.05% surfactant P20; pH 7.4) supplemented with 10 mM CaCl$_2$. Recombinant HIV-1(III$_B$) gp120

(ImmunoDiagnostics Inc., Woburn, MA), recombinant HIV-1(HxB2) gp41 (Acris Antibodies GmbH, Herford, Germany) and human serum albumin (HSA) (Sigma) were covalently immobilized on a CM5 sensor chip in 10 mM sodium acetate, pH 4, using standard amine coupling chemistry, resulting in chip densities of respectively 3531, 3091 and 3333 RU. A reference flow cell was used as a control for non-specific binding and refractive index changes. Samples were injected for 2 min at a flow rate of 45 μl/min and followed by a dissociation phase of 2 min. The CM5 sensor chip surface was regenerated with a single injection of Glycine–HCl pH = 3.

4.9. HIV-1 reverse transcriptase assay

Enzyme reactions (50 μL in volume) were carried out in a 50 mM Tris–HCl (pH 7.8) buffer that contained 5 mM dithiothreitol, 300 mM glutathione, 0.5 mM EDTA, 150 mM KCl, 5 mM MgCl$_2$, 1.25 μg of bovine serum albumin, 0.06% Triton X-100, an appropriate concentration of 2.8 μM [^{3}H]dGTP (2 μCi/assay), varying concentrations of the test compounds, and a fixed concentration of poly(rC)/oligo(dG) (0.1 mM). Reactions were initiated by the addition of 1 μL of wild-type or mutant RT and were incubated for 30 min at 37 °C. Reactions were terminated by the addition of 200 μL of 2 mg/mL yeast RNA, 2 mL of 0.1 M Na$_4$P$_2$O$_7$ (in 1 M HCl), and 2 mL of 10% (v/v) trichloroacetic acid. The solutions were kept on ice for 30 min, after which the acid-insoluble material was washed and analyzed for radioactivity.

Acknowledgments

Supplementary data

Supplementary data associated with this article can be found, in the online version, at http://dx.doi.org/10.1016/j.bmc.2013.12.051.

References and notes

1. Nimjee, S. M.; Rusconi, C. P.; Sullenger, B. A. Annu. Rev. Med. 2005, 56, 555.
2. Famulok, M.; Mayer, G. ChemBioChem 2005, 6, 19.
3. Proske, D.; Blank, M.; Buhmann, R.; Resch, A. Appl. Microbiol. Biotechnol. 2005, 69, 367.
4. Hermann, T.; Patel, D. J. Science 2000, 287, 820.
5. Doluca, O.; Withers, J. M.; Filichev, V. V. Chem. Rev. 2013, 113, 3044.
6. Tucker, W. O.; Shum, K. T.; Tanner, J. A. Curr. Pharm. Des. 2012, 8, 2014.
7. Spindler, I.; Fritzsche, W. Guanine Quartets: Structure and Application; Royal Society of Chemistry: London, 2012.
8. Neidle, S. Therapeutic Applications of Quadruplex Nucleic Acids; Academic Press Elsevier: Oxford (UK), 2012.
9. Navani, N. K.; Li, Y. Curr. Opin. Chem. Biol. 2006, 10, 272.
10. White, R. R.; Sullenger, B. A.; Rusconi, C. P. J. Clin. Invest. 2000, 106, 929.
11. Chou, S.-H.; Chin, K.-H.; Wang, A. H.-J. Trends Biochem. Sci. 2005, 30, 231. and references therein cited.
12. Urata, H.; Kumashiro, T.; Kawahata, T.; Otake, T.; Akagi, M. Biochem. Biophys. Res. Commun. 2004, 313, 55.
13. Jing, N.; De Clercq, E.; Randoi, R. F.; Pallansch, L.; Lackman-Smith, C.; Lee, S.; Hogan, M. E. J. Biol. Chem. 2000, 275, 3421.
14. Jing, N.; Marchand, C.; Liu, J.; Mitra, R.; Hogan, M. E.; Pommier, Y. J. Biol. Chem. 2000, 275, 21460.
15. Este, J. A.; Cabrera, C.; Schols, D.; Cherepanov, P.; Gutierrez, A.; Witvrouw, M.; Pannecouque, C.; Debyser, Z.; Rando, R. F.; Clotet, B.; Desmyter, J.; De Clercq, E. Mol. Pharmacol. 1998, 53, 340.
16. Wyatt, J. R.; Vickers, T. A.; Roberson, J. L.; Buckheit, R. W.; Klimkait, T., Jr; DeBaets, E.; Davis, P. W.; Rayner, B.; Imbach, J. L.; Ecker, D. J. Proc. Natl. Acad. Sci. 1994, 91, 1356.
17. Chang, G. P.; Masad, J. D. Nucleic Acids Res. 2007, 35, 4977.
18. Phan, A. T.; Kuryavyi, V.; Ma, J. B.; Faure, A.; Andréola, M. L.; Patel, D. J. Proc. Natl. Acad. Sci. U.S.A. 2005, 102, 634.
19. Suzuki, J.; Miyano-Kurosaki, N.; Kuwasaki, T.; Takeuchi, H.; Kawai, G.; Takaku, H. J. Virol. 2002, 76, 3015.
20. de Soultrait, V. R.; Lozach, P.-Y.; Altmeyer, R.; Tarrago-Litvak, L.; Litvak, S.; Andréola, M. L. J. Mol. Biol. 2002, 324, 195.
21. Esté, J. A.; Cabrera, C.; Schols, D.; Cherepanov, P.; Gutierrez, A.; Witvrouw, M.; Pannecouque, C.; Debyser, Z.; Rando, R. F.; Clotet, B.; Desmyter, J.; De Clercq, E. Mol. Pharmacol. 1998, 53, 340.
22. Jing, N.; Hogan, M. E. J. Biol. Chem. 1998, 273, 34992.
23. Jing, N.; Rando, R. F.; Pommier, Y.; Hogan, M. E. Biochemistry 1997, 36, 12498.
24. Mazumder, A.; Neamati, N.; Ojwang, J. O.; Sunder, S.; Rando, R. F.; Pommier, Y. Biochemistry 1996, 35, 13762.
25. Wyatt, J. R.; Vicker, T. A.; Roberson, J. L.; Buckheit, J. R. W.; Klimkait, T.; DeBaets, E.; Davis, P. W.; Rayner, B.; Imbach, J. L.; Ecker, D. J. Proc. Natl. Acad. Sci. U.S.A. 1994, 91, 1356.
26. Hotoda, H.; Koizumi, M.; Koga, R.; Kaneko, M.; Momota, K.; Ohmine, T.; Furukawa, H.; Agatsuma, T.; Nishigaki, T.; Sone, J. J. Med. Chem. 1998, 41, 3655.
27. Koizumi, M.; Koga, R.; Hotoda, H.; Momota, K.; Ohmine, T.; Furukawa, H.; Agatsuma, T.; Nishigaki, T.; Abe, K.; Kosaka, T.; Tsutsumi, S.; Sone, J.; Kaneko, M.; Kimura, S.; Shimada, K. Bioorg. Med. Chem. Lett. 1997, 5, 2235.
28. Hotoda, H.; Koizumi, M.; Koga, R.; Momota, K.; Ohmine, T.; Furukawa, H.; Nishigaki, T.; Kinoshita, T.; Kaneko, M. Nucleosides Nucleotides 1996, 15, 531.
29. D'Atri, V.; Oliviero, G.; Amato, J.; Borbone, N.; D'Errico, S.; Mayol, L.; Piccialli, V.; Haider, S.; Hoorelbeke, B.; Balzarini, J.; Piccialli, G. Chem. Commun. 2012, 9516.
30. Pedersen, E. B.; Nielsen, J. T.; Nielsen, C.; Filichev, V. V. Nucleic Acids Res. 2011, 39, 2470.
31. Chen, W.; Xu, L.; Cai, L.; Zheng, B.; Wang, K.; He, J.; Liu, K. Bioorg. Med. Chem. Lett. 2011, 21, 5762.
32. Oliviero, G.; Amato, J.; Borbone, N.; D'Errico, S.; Galeone, A.; Mayol, L.; Haider, S.; Olubiyi, O.; Hoorelbeke, B.; Balzarini, J.; Piccialli, G. Chem. Commun. 2010, 8971.
33. D'Onofrio, J.; Petraccone, L.; Erra, E.; Martino, L.; Di Fabio, G.; De Napoli, L.; Giancola, C.; Montesarchio, D. Bioconjugate Chem. 2007, 18, 1194.
34. D'Onofrio, J.; Petraccone, L.; Erra, E.; Martino, L.; Di Fabio, G.; Iadonisi, A.; Balzarini, J.; Giancola, C.; Montesarchio, D. Bioconjugate Chem. 2008, 19, 607.
35. Di Fabio, G.; D'Onofrio, J.; Chiapparelli, M.; Hoorelbeke, M.; Montesarchio, D.; Balzarini, J.; De Napoli, L. Chem. Commun. 2011, 2363.
36. Chillemi, R.; Greco, V.; Nicoletti, V. G.; Sciuto, S. Bioconjugate Chem. 2013, 24, 648. and references therein cited.
37. Raouane, M.; Desmaële, D.; Urbinati, G.; Massaad-Massade, L.; Couvreur, P. Bioconjugate Chem. 2012, 23, 1091.
38. Laing, B. M.; Barrow-Laing, L.; Harrington, M.; Long, E. C.; Bergstrom, D. E. Bioconjugate Chem. 2010, 21, 1537.
39. Jayawickramarajah, J.; Tagore, D. M.; Tsou, L. K.; Hamilton, A. D. Angew. Chem., Int. Ed. 2007, 46, 7583. and references therein cited.
40. Brown, T.; Brown, D. J. S. Modern machine-aided methods of oligodeoxyribonucleotide synthesis. In Oligonucleotides and Analogues: A Practical Approach; Daniel, E., Ed.; IRL Press: Oxford, UK, 1991; pp 1–23.
41. Paramasivan, S.; Rujan, I.; Bolton, P. H. Methods 2007, 43, 324.
42. Petraccone, L.; Spink, C. O.; Trent, J.; Garbett, N. C.; Mekmaysy, C. S.; Giancola, C.; Chaires, J. B. J. Am. Chem. Soc. 2011, 133, 20951.
43. Šket, P.; Plavec, J. J. Am. Chem. Soc. 2010, 132, 12724.
44. Antonacci, C.; Chaires, J. B.; Sheardy, R. D. Biochemistry 2007, 46, 4654.
45. Chaires, J. B. FEBS J. 2010, 277, 1098.
46. Park, K. J. Control. Release 2012, 157, 3.
47. Elsadek, B.; Kratz, F. J. Control Release 2012, 157, 4. and references therein cited.
48. Grasso, D.; La Rosa, C.; Milardi, D.; Fasone, S. Thermochim. Acta 1995, 265, 163.
49. Palmieri, M.; Malgieri, G.; Russo, L.; Baglivo, I.; Esposito, S.; Netti, F.; Del Gatto, A.; de Paola, I.; Zaccaro, L. P. V.; Isernia, C.; Milardi, D.; Fattorusso, R. J. Am. Chem. Soc. 2013, 135, 5220.
50. Arena, G.; Fattorusso, R.; Grasso, G.; Grasso, G. I.; Isernia, C.; Malgieri, G.; Milardi, D.; Rizzarelli, E. Chem. Eur. J. 2011, 17, 11596.
51. Milardi, D.; Arnesano, F.; Grasso, G.; Magrì, A.; Tabbì, G.; Scintilla, S.; Natile, G.; Rizzarelli, E. Angew. Chem., Int. Ed. 2007, 46, 7993.